Arch. Mech., **67**, 5, pp. 355–370, Warszawa 2015

Surface effects on the wave propagation in composites with random dispersive parallel cylindrical nanofibers

Z. KONG[1)], F. W. QIANG[1)], P. J. WEI[1),2)], Q. TANG[2)]

[1)] *Department of Applied Mechanics*
University of Science and Technology Beijing
Beijing 100083, China
e-mail: weipj@ustb.edu.cn

[2)] *State Key Laboratory of Nonlinear Mechanics (LNM)*
Chinese Academy of Science, Beijing
Beijing 100080, China

The propagation of elastic waves in composites with randomly distributed parallel cylindrical nanofibers is studied. The non-classical boundary conditions on the surface of nanofibers are derived by using the surface elasticity theory. The scattering waves from an individual nanofiber are obtained by the plane-wave expansion method. These scattering waves from all nanofibers are summed up to obtain the multiple-scattering waves. The effective propagation constants (speed and attenuation) of coherent waves and the associated effective dynamical moduli of composites are evaluated numerically. Based on these numerical results, the influences of the surface effects on the effective dynamical properties of composites are discussed.

Key words: multiple scattering, effective speed, effective moduli, nanofiber, surface stress.

1. Introduction

The propagation of elastic waves in composites with randomly distributed cylindrical fibers is of great importance in both theoretical and application aspects, e.g., the measure of elastic constants, the nondestructive testing of damage and the designing of advanced composite material [1–5]. Bose and Mal [6–8] studied the propagation of anti-plane axial shear wave (SH-wave), in-plane longitudinal wave (P-wave) and shear-vertical (SV-wave) in a fiber-reinforced composite, where the circular fibers are assumed to be parallel to each other and randomly distributed with a statistically uniform distribution. Yang and Mal [9] studied the same problem and gave a formula to estimate the effective wavenumber. Shindo and Niwa [10] and Shindo *et al.* [11] studied the multiple

scattering waves in a metal matrix composite reinforced by dispersive parallel fibers with interfacial layer.

Wei and Huang [12] and Wei [13] studied further the wave propagation in the composites with random distributed spherical inclusions. The effective propagation constants of coherent waves and the dynamical effective moduli of composites are estimated by making use of an effective field method and an effective medium method. In the scattering problem based on classical elasticity theory, the contribution from surface stress or interface stress is usually neglected because the surface or interface is limited to only a few atomic or molecular layers and the surface stress or interface stress is very small when compared with the bulk stress. When the radius of fibers shrinks to nanoscales with the volume fraction fixed, the surface or interface stress may have significant effects on the scattering waves. Based on the surface elasticity theory established by Gurtin and Murdoch [14], Ru *et al.* [15] investigated the diffractions of elastic waves from an individual nanosized cylindrical inclusion and showed the obvious importance of surface effects on the dynamic stress intensity around the inclusion. Recently, the effective propagation constants of coherent SH-wave in nanocomposites material with dispersive parallel cylindrical nanofibers were studied in [16].

Hasheminejad and Avazmohammadi [17] also studied the effective dynamic properties of unidirectional nanofiber-reinforced composites based on the generalized self-consistent multiple scattering approach. Their investigation showed that the effect of interface stress is evident and this effect gradually diminishes as the fiber size increases. However, the effective wavenumber formulas used in [16, 17] are essentially the elastic version of the single formula for acoustics waves. It was shown by Linton and Martin [18] that these formulas are actually incorrect. A modified form of the effective wavenumber equation for acoustics was derived by Linton and Martin [18] using other methods. The elastic version of the corrected Linton–Martin formula was recently given by Conoir and Norris [19]. In their formula, the contributions from the mode conversions between P- and SV-waves are taken into consideration.

In the present work, the surface stresses of nanofibers are considered to obtain the nontraditional interface conditions between the nanofibers and the host material. Based on the interface conditions, the individual scattering waves and the multiple scattering waves thus include the surface effects of nanofibers; the effective propagation constants of coherent waves and the associated effective dynamic moduli of the nanofiber-reinforced composites are estimated numerically by using the corrected Linton–Martin formula. The influences of surface/interface effects of nanofibers are discussed based on the numerical results.

2. The individual scattering of a nanofiber

Consider a cylindrical nanofiber of radius a embedded in an isotropic infinite host material, see Fig. 1; (x, y, z) is the right-handed Cartesian coordinate system and the $z$axis along the central axis of cylindrical nanofiber; (r, θ, z) is the corresponding cylindrical coordinate with θ being measured from the positive direction of x axis. The scattering problems of incident P-wave and SV-wave are considered.

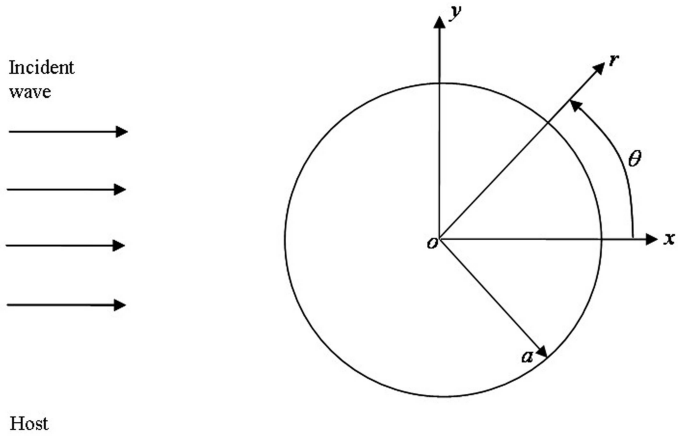

FIG. 1. The individual scattering of a nanofiber.

In the surface elasticity theory, a surface is regarded as a negligibly thin layer adhered to the bulk without slipping and having different elastic constants with the host and the fiber. In the host and the fiber, the classical theory of elasticity holds. The motion equation without body force and the constitutive equation are given in [14, 20]

$$\sigma^b_{ij,j} = \rho^b \ddot{u}^b_i, \qquad \sigma^b_{ij} = \lambda^b \varepsilon^b_{kk}\delta_{ij} + 2\mu^b \varepsilon^b_{ij}, \tag{2.1}$$

$$\sigma^f_{ij,j} = \rho^f \ddot{u}^f_i, \qquad \sigma^f_{ij} = \lambda^f \varepsilon^f_{kk}\delta_{ij} + 2\mu^f \varepsilon^f_{ij}, \tag{2.2}$$

where Einstein's summation convention is adopted, δ_{ij} is the Kronecker delta, the Latin subscripts i, j and k range over the coordinates r, θ and z. The elastic Lame constants and the mass density are λ, μ and ρ, respectively. The superscript b indicates the bulk and the superscript f indicates the fiber, u_i, σ_{ij} and ε_{ij} are the displacement vector, the stress tensor and the strain tensor, respectively.

The interface tension $\sigma^s_{\alpha\beta}$ is related to the interface energy density Γ as [14]

$$\sigma^s_{\alpha\beta} = \delta_{\alpha\beta} + \frac{\partial \Gamma}{\partial \varepsilon_{\alpha\beta}}, \tag{2.3}$$

where the superscript s indicates the surface, and the Greek subscripts α, β and γ range over the coordinates z and θ. For an isotropic interface, they can be expressed distinctly as [14]

$$\sigma^s_{\alpha\beta} = \sigma^0\delta_{\alpha\beta} + 2(\mu^s - \sigma^0)\varepsilon_{\alpha\beta} + (\lambda^s + \sigma^0)\varepsilon_{\gamma\gamma}\delta_{\alpha\beta} + \sigma^0 u_{\alpha,\beta}, \tag{2.4}$$

where σ^0 is the residual stress tension under unstrained condition, λ^s and μ^s are the elastic Lame constants of interface and are of the dimension $\mathrm{N/m^{-1}}$. In a more comprehensive model of the surface/interface, the surface/interface has not only own elastic properties but also own inertia and even flexural stiffness, e.g., see STEIGMANN and OGDEN [21] and LUCA *et al.* [22]. In the present work, the inertia and the flexural stiffness of surface are neglected based on the fact that the thin layer is composed by only a few atomic or molecular layers. The problem is greatly simplified by such treatment. The existence of surface stresses and the hypothesis that surface adheres perfectly to the bulk without slipping lead to a set of nonclassical boundary conditions

$$u^b_i = u^s_i = u^f_i, \tag{2.5}$$

$$\sigma^b_{r\alpha} - \sigma^f_{r\alpha} = -\sigma^s_{\beta\alpha,\beta}, \qquad \sigma^b_{rr} - \sigma^f_{rr} = \sigma^s_{\alpha\beta}\kappa_{\alpha\beta}, \tag{2.6}$$

where $\kappa_{\alpha\beta}$is the curvature tensor of surface. In the case of incident P- and SV-waves, the scattering waves in a cylindrical nanofiber include both P- and SV-waves. The incident and scattered P- and SV-waves are polarized in oxy plane. To achieve the decoupling purpose, the displacement potentials ϕ and ψ are usually introduced, namely, $\mathbf{u} = \nabla\phi + \nabla\times\psi\mathbf{e}_z$. The governing equations (2.1) require

$$\nabla^2\phi + k_p^2\phi = 0, \tag{2.7}$$

$$\nabla^2\psi + k_{sv}^2\psi = 0. \tag{2.8}$$

The solution of Eqs. (2.7) and (2.8) is a combination of a series of cylindrical wave functions. Therefore, the incident wave, the scattered wave in the host and the transmitted wave in the fiber can be expressed as

$$\begin{aligned}\phi^i &= \phi_0 e^{i(k_p^b x - \omega t)} + \psi_0 e^{i(k_{sv}^b x - \omega t)} \\ &= \phi_0 \sum_{m=-\infty}^{\infty} i^m J_m(k_p^b r) e^{i(m\theta - \omega t)} + \psi_0 \sum_{m=-\infty}^{\infty} i^m J_m(k_{sv}^b r) e^{i(m\theta - \omega t)},\end{aligned} \tag{2.9}$$

$$\begin{aligned}\phi^r &= \sum_{m=-\infty}^{\infty} B_m H_m^{(1)}(k_p^b r) e^{i(m\theta - \omega t)}, \\ \psi^r &= \sum_{m=-\infty}^{\infty} C_m H_m^{(1)}(k_{sv}^b r) e^{i(m\theta - \omega t)},\end{aligned} \tag{2.10}$$

$$
\begin{aligned}
\phi^f &= \sum_{m=-\infty}^{\infty} b_m J_m(k_p^f r) e^{i(m\theta-\omega t)}, \\
\psi^f &= \sum_{m=-\infty}^{\infty} c_m J_m(k_{sv}^f r) e^{i(m\theta-\omega t)},
\end{aligned} \tag{2.11}
$$

where ϕ_0 and ψ_0 are the amplitudes of incident wave. $J_n(kr)$ is the cylindrical Bessel function and $H_n^{(1)}(kr)$ is the cylindrical Hankel function. B_m, C_m, b_m and c_m are the unknown coefficients to be determined by boundary conditions, i.e., Eqs. (2.5) and (2.6), k_p^b, k_{sv}^b, k_p^f and k_{sv}^f are the wavenumbers of P- and SV-waves in the host and in the fiber, respectively. The time factor $e^{-i\omega t}$ is neglected in the following formulations. The displacement components in the host and the fiber are, respectively,

$$
\begin{aligned}
u_r^b &= \frac{\partial(\phi^i+\phi^r)}{\partial r}+\frac{1}{r}\frac{\partial(\psi^i+\psi^r)}{\partial r} \\
&= \frac{1}{r}\sum_{m=-\infty}^{\infty}[\phi_0 i^m E_{11}^{bi}(r)+B_m E_{11}^{br}(r)+\psi_0 i^m E_{12}^{bi}(r)+C_m E_{12}^{br}(r)]e^{im\theta},
\end{aligned} \tag{2.12}
$$

$$
u_r^f = \frac{\partial\phi^f}{\partial r}+\frac{1}{r}\frac{\partial\psi^f}{\partial r} = \frac{1}{r}\sum_{m=-\infty}^{\infty}[b_m E_{21}^{fi}(r)+c_m E_{22}^{fi}(r)]e^{im\theta}, \tag{2.13}
$$

$$
\begin{aligned}
u_\theta^b &= \frac{1}{r}\frac{\partial(\phi^i+\phi^r)}{\partial\theta}-\frac{\partial(\psi^i+\psi^r)}{\partial r} \\
&= \frac{1}{r}\sum_{m=-\infty}^{\infty}[\phi_0 i^m E_{31}^{bi}(r)+B_m E_{31}^{br}(r)-\psi_0 i^m E_{32}^{bi}(r)-C_m E_{32}^{br}(r)]e^{im\theta},
\end{aligned} \tag{2.14}
$$

$$
\begin{aligned}
u_\theta^f &= \frac{1}{r}\frac{\partial\phi^f}{\partial\theta}-\frac{\partial\psi^f}{\partial r} \\
&= \frac{1}{r}\sum_{m=-\infty}^{\infty}[b_m E_{41}^{fi}(r)-c_m E_{42}^{fi}(r)]e^{im\theta},
\end{aligned} \tag{2.15}
$$

where

$$
\begin{aligned}
E_{11}^{bi}(r) &= k_p^b r J_{m-1}(k_p^b r) - m J_m(k_p^b r), \\
E_{12}^{bi}(r) &= im J_m(k_{sv}^b r), \\
E_{21}^{fi}(r) &= k_p^f r J_{m-1}(k_p^f r) - m J_m(k_p^f r), \\
E_{22}^{fi}(r) &= im J_m(k_{sv}^f r), \\
E_{31}^{bi}(r) &= im J_m(k_p^b r), \\
E_{32}^{bi}(r) &= k_{sv}^b r J_{m-1}(k_{sv}^b r) - m J_m(k_{sv}^b r),
\end{aligned}
$$

$$E_{41}^{fi}(r) = imJ_m(k_p^f r),$$
$$E_{42}^{fi}(r) = k_{sv}^f r J_{m-1}(k_{sv}^f r) - mJ_m(k_{sv}^f r).$$

$E_{11}^{br}(r)$, $E_{12}^{br}(r)$, $E_{31}^{br}(r)$ and $E_{32}^{br}(r)$ are obtained by replacing $J_m(kr)$ by $H_m^{(1)}(kr)$ in the expressions of $E_{11}^{bi}(r)$, $E_{12}^{bi}(r)$, $E_{31}^{bi}(r)$ and $E_{32}^{bi}(r)$, respectively.

Further, the stress components in the host, the fiber and the interface can be obtained, respectively,

$$\sigma_{rr}^b = \lambda^b \nabla^2(\phi^i + \phi^r) + 2\mu^b \left[\frac{\partial^2(\phi^i + \phi^r)}{\partial r^2} + \frac{\partial}{\partial r}\left(\frac{1}{r} \frac{\partial(\psi^i + \psi^r)}{\partial \theta} \right) \right] \tag{2.16}$$
$$= \frac{2\mu^b}{r^2} \sum_{m=-\infty}^{\infty} [\phi_0 i^m E_{51}^{bi}(r) + B_m E_{51}^{br}(r) + \psi_0 i^m E_{52}^{bi}(r) + C_m E_{52}^{br}(r)] e^{im\theta},$$

$$\sigma_{rr}^f = \lambda^b \nabla^2 \phi^f + 2\mu^b \left[\frac{\partial^2 \phi^f}{\partial r^2} + \frac{\partial}{\partial r}\left(\frac{1}{r} \frac{\partial \psi^f}{\partial \theta} \right) \right] \tag{2.17}$$
$$= \frac{2\mu^f}{r^2} \sum_{m=-\infty}^{\infty} [b_m E_{51}^{fi}(r) + c_m E_{52}^{fi}(r)] e^{im\theta},$$

$$\sigma_{r\theta}^b = \mu^b \left[\frac{2}{r} \frac{\partial^2(\phi^i + \phi^r)}{\partial \theta \partial r} - \frac{2}{r^2} \frac{\partial(\phi^i + \phi^r)}{\partial \theta} \right. \tag{2.18}$$
$$\left. + \frac{1}{r^2} \frac{\partial^2(\psi^i + \psi^r)}{\partial \theta^2} - r \frac{\partial}{\partial r}\left(\frac{1}{r} \frac{\partial(\psi^i + \psi^r)}{\partial r} \right) \right]$$
$$= \frac{2\mu^b}{r^2} \sum_{m=-\infty}^{\infty} [\phi_0 i^m E_{71}^{bi}(r) + B_m E_{71}^{br}(r) + \psi_0 i^m E_{72}^{bi}(r) + C_m E_{72}^{br}(r)] e^{im\theta},$$

$$\sigma_{r\theta}^f = \mu^f \left[\frac{2}{r} \frac{\partial^2 \phi^f}{\partial \theta \partial r} - \frac{2}{r^2} \frac{\partial \phi^f}{\partial \theta} + \frac{1}{r^2} \frac{\partial^2 \psi^f}{\partial \theta^2} - r \frac{\partial}{\partial r}\left(\frac{1}{r} \frac{\partial \psi^f}{\partial r} \right) \right] \tag{2.19}$$
$$= \frac{2\mu^f}{r^2} \sum_{m=-\infty}^{\infty} [b_m E_{71}^{fi}(r) + c_m E_{72}^{fi}(r)] e^{im\theta},$$

$$\sigma_{\theta\theta}^s = \sigma^0 + (\lambda^s + 2\mu^s)\varepsilon_{\theta\theta}^s \tag{2.20}$$
$$= \sigma^0 + \frac{(\lambda^s + 2\mu^s)}{r^2}$$
$$\times \sum_{m=-\infty}^{\infty} [\phi_0 i^m E_{61}^{si}(r) + B_m E_{61}^{sr}(r) + \psi_0 i^m E_{62}^{si}(r) + C_m E_{62}^{sr}(r)] e^{im\theta},$$

where

$$E_{51}^{bi}(r) = \left[m^2 + m - \left(\frac{\lambda^b + 2\mu^b}{2\mu^b} \right) (k_p^b r)^2 \right] J_m(k_p^b r) - k_p^b r J_{m-1}(k_p^b r),$$
$$E_{52}^{bi}(r) = \mathrm{i}\, mk_{sv}^b r J_{m-1}(k_{sv}^b r) - (\mathrm{i}\, m^2 + im) J_m(k_{sv}^b r),$$

$$E_{51}^{fi}(r) = \left[m^2 + m - \left(\frac{\lambda^f + 2\mu^f}{2\mu^f}\right)(k_p^f r)^2\right] J_m(k_p^f r) - k_p^f r J_{m-1}(k_p^f r),$$
$$E_{52}^{fi}(r) = \mathrm{i}\, m k_{sv}^f r J_{m-1}(k_{sv}^f r) - (\mathrm{i}\, m^2 + \mathrm{i}\, m) J_m(k_{sv}^f r),$$
$$E_{61}^{si}(r) = k_p^b r J_{m-1}(k_p^b r) - (m^2 + m) J_m(k_p^b r),$$
$$E_{62}^{si}(r) = (\mathrm{i}\, m^2 + \mathrm{i}\, m) J_m(k_{sv}^b r) - \mathrm{i}\, m k_{sv}^b r J_{m-1}(k_{sv}^b r),$$
$$E_{71}^{bi}(r) = \mathrm{i}\, m k_p^b r J_{m-1}(k_p^b r) - (\mathrm{i}\, m^2 + \mathrm{i}\, m) J_m(k_p^b r),$$
$$E_{72}^{bi}(r) = \left[\frac{(k_{sv}^b r)^2}{2} - m^2 - m\right] J_m(k_{sv}^b r) + k_{sv}^b r J_{m-1}(k_{sv}^b r),$$
$$E_{71}^{fi}(r) = \mathrm{i}\, m k_p^f r J_{m-1}(k_p^f r) - (\mathrm{i}\, m^2 + \mathrm{i}\, m) J_m(k_p^f r),$$
$$E_{72}^{fi}(r) = \left[\frac{(k_{sv}^f r)^2}{2} - m^2 - m\right] J_m(k_{sv}^f r) + k_{sv}^f r J_{m-1}(k_{sv}^f r).$$

$E_{51}^{br}(r)$, $E_{52}^{br}(r)$, $E_{61}^{sr}(r)$, $E_{62}^{sr}(r)$, $E_{71}^{br}(r)$ and $E_{72}^{br}(r)$ are obtained by replacing $J_m(kr)$ by $H_m^{(1)}(kr)$ in the expressions of $E_{51}^{bi}(r)$, $E_{52}^{bi}(r)$,$E_{61}^{si}(r)$, $E_{62}^{si}(r)$, $E_{71}^{bi}(r)$ and $E_{72}^{bi}(r)$, respectively.

The boundary condition equations (2.5) and (2.6) can be explicitly expressed in the cylindrical coordinates as

$$u_r^b\big|_{r=a} = u_r^f\big|_{r=a} = u_r^s, \tag{2.21}$$
$$u_\theta^b\big|_{r=a} = u_\theta^f\big|_{r=a} = u_\theta^s, \tag{2.22}$$
$$\sigma_{rr}^b\big|_{r=a} - \sigma_{rr}^f\big|_{r=a} = \frac{\sigma_{\theta\theta}^s}{a}, \tag{2.23}$$
$$\sigma_{r\theta}^b\big|_{r=a} - \sigma_{r\theta}^f\big|_{r=a} = -\frac{\partial \sigma_{\theta\theta}^s}{a\partial\theta}. \tag{2.24}$$

Inserting Eqs. (2.12)–(2.15) and Eqs. (2.16)–(2.20) into Eqs. (2.21) and (2.22) and Eqs. (2.23) and (2.24) leads to

$$\begin{bmatrix} E_{11}^{br}(a) & E_{12}^{br}(a) & -E_{21}^{fi}(a) & -E_{22}^{fi}(a) \\ E_{31}^{br}(a) & -E_{32}^{br}(a) & -E_{41}^{fi}(a) & E_{42}^{fi}(a) \\ E_{51}^{br}(a) - S_1 E_{61}^{sr}(a) & E_{52}^{br}(a) - S_1 E_{62}^{sr}(a) & -g E_{51}^{fi}(a) & -g E_{52}^{fi}(a) \\ E_{71}^{br}(a) + imS_1 E_{61}^{sr}(a) & E_{72}^{br}(a) + imS_1 E_{62}^{sr}(a) & -g E_{71}^{fi}(a) & -g E_{72}^{fi}(a) \end{bmatrix} \begin{bmatrix} B_m \\ C_m \\ b_m \\ c_m \end{bmatrix} \tag{2.25}$$
$$= \begin{bmatrix} -\phi_0 i^m E_{11}^{bi}(a) - \psi_0 i^m E_{12}^{bi}(a) \\ -\phi_0 i^m E_{31}^{bi}(a) + \psi_0 i^m E_{32}^{bi}(a) \\ -\phi_0 i^m (E_{51}^{bi}(a) - S_1 E_{61}^{si}(a)) - \psi_0 i^m (E_{52}^{bi}(a) - S_1 E_{62}^{si}(a)) \\ -\phi_0 i^m (E_{71}^{bi}(a) + imS_1 E_{61}^{si}(a)) - \psi_0 i^m (E_{72}^{bi}(a) + imS_1 E_{62}^{si}(a)) \end{bmatrix} + S_2 \delta_{m0} \begin{bmatrix} 0 \\ 0 \\ 1 \\ 0 \end{bmatrix},$$

where

$$g = \frac{\mu^f}{\mu^b}, \qquad S_1 = \frac{(\lambda^s + 2\mu^s)}{2\mu^b a} \qquad \text{and} \qquad S_2 = \frac{\sigma^0 a}{2\mu^b}$$

are the surface parameters which stand for the surface effects. When $S_1 = S_2 = 0$, Eq. (2.25) reduces to the traditional interface condition. The unknown coefficient B_m and C_m of the scattered wave can be obtained by solving Eq. (2.25).

3. The multiple scattering waves from all nanofibers

Consider N parallel cylindrical fibers randomly distributed in an isotropic elastic medium. The positions of these fibers are defined by the variable set $(\mathbf{r}_1, \mathbf{r}_2, \ldots, \mathbf{r}_N)$ which represents a particular configuration of these fibers. The joint probability distribution of this configuration is denoted by $p(\mathbf{r}_1, \mathbf{r}_2, \ldots, \mathbf{r}_N)$, and stands for the probability of finding these fibers in the configuration. In the composite material, the total wave field at any point $\mathbf{r}$ outside all fibers can be expressed in the multiple scattering form

$$\begin{aligned}(3.1)\qquad &\mathbf{u}(\mathbf{r}; \mathbf{r}_1, \mathbf{r}_2, \ldots, \mathbf{r}_N)\\ &= \mathbf{u}^i(\mathbf{r}) + \sum_{k=1}^{N} \mathbf{T}^s(\mathbf{r}_k)\mathbf{u}^i(\mathbf{r}) + \sum_{m=1}^{N} \mathbf{T}^s(\mathbf{r}_m) \sum_{k=1, k\neq m}^{N} \mathbf{T}^s(\mathbf{r}_k)\mathbf{u}^i(\mathbf{r}) + \cdots,\end{aligned}$$

where $\mathbf{T}^s(\mathbf{r}_k)$ is the scattering operator which transforms the incident wave into the scattered wave. The first term in Eq. (3.1) represents the incident wave. The second term represents a first scattering wave of the incident wave. The third term represents a second scattering wave of the incident wave and so on. The configurational average of total wave field

$$(3.2)\qquad \langle \mathbf{u}(\mathbf{r}; \mathbf{r}_1, \ldots, \mathbf{r}_N) \rangle = \int \ldots \int \mathbf{u}(\mathbf{r}; \mathbf{r}_1, \cdots, \mathbf{r}_N) p(\mathbf{r}_1, \ldots, \mathbf{r}_N) dV_1 \cdots dV_N$$

is defined as the coherent waves or averaged waves. The effective propagation constants of the coherent waves were studied incessantly in the past several decades. For the acoustic wave, the early formula is in the following form:

$$(3.3)\qquad (k^*)^2 = k^2 + \delta_1 n,$$

where k is the wavenumber in the host while k^* is the effective wavenumber in the composites and n is the number density of fibers and is related to the volume fraction c by $n = c/(\pi a^2)$. LINTON and MARTIN [18] gave a second-order correction formula

$$(3.4)\qquad (k^*)^2 = k^2 + \delta_1 n + \delta_2 n^2.$$

However, there is some controversy over the proper value for δ_2. In general, δ_1 and δ_2 are the functions of the far-field individual scatterer form. YANG and MAL [9] gave a formula of effective wavenumber for the elastic waves in the fiber-reinforced random composites

$$\left(\frac{k_p^*}{k_p^b}\right)^2 = \left[1 - \frac{i2n}{(k_p^b)^2} f_p(0)\right]^2 - \left[\frac{i2n}{(k_p^b)^2} f_p(\pi)\right]^2, \tag{3.5}$$

$$\left(\frac{k_{sv}^*}{k_{sv}^b}\right)^2 = \left[1 - \frac{i2n}{(k_{sv}^b)^2} f_{sv}(0)\right]^2 - \left[\frac{i2n}{(k_{sv}^b)^2} f_{sv}(\pi)\right]^2, \tag{3.6}$$

where $f_q(0)$ $(q = p, sv)$ and $f_q(\pi)$ $(q = p, sv)$ are the forward scattering amplitude and the backward scattering amplitude, respectively. Equations (3.5) and (3.6) were used in [16, 17]. However, it was shown by LINTON and MARTIN [18] that this is actually incorrect, because the contributions from the mode conversions between P- and SV-waves are not taken into consideration. A modified form of the effective wavenumber equation for the elastic waves has been recently given by CONOIR and NORRIS [19]

$$\begin{aligned}\left(\frac{k_p^*}{k_p^b}\right)^2 = 1 &- \frac{4\mathrm{i}\, n f_{pp}(0)}{(k_p^b)^2} + \frac{8n^2}{\pi (k_p^b)^4} \int_0^{2\pi} d\theta \cot\left(\frac{\theta}{2}\right) \frac{d}{d\theta}[f_{pp}(\theta) f_{pp}(-\theta)] \\ &+ \frac{8n^2}{\pi (k_p^b)^4} \int_0^{\pi} d\theta \frac{f_{ps}(\theta) f_{sp}(-\theta) + f_{sp}(\theta) f_{ps}(-\theta)}{\kappa^2 - 2\kappa \cos(\theta) + 1},\end{aligned} \tag{3.7}$$

$$\begin{aligned}\left(\frac{k_{sv}^*}{k_{sv}^b}\right)^2 = 1 &- \frac{4\mathrm{i}\, n f_{ss}(0)}{(k_{sv}^b)^2} + \frac{8n^2}{\pi (k_{sv}^b)^4} \int_0^{2\pi} d\theta \cot\left(\frac{\theta}{2}\right) \frac{d}{d\theta}[f_{ss}(\theta) f_{ss}(-\theta)] \\ &+ \frac{8n^2}{\pi (k_{sv}^b)^4} \int_0^{\pi} d\theta \frac{f_{ps}(\theta) f_{sp}(-\theta) + f_{sp}(\theta) f_{ps}(-\theta)}{(1 - 2/\kappa \cos(\theta) + 1/\kappa^2)} \\ &- \frac{16n^2}{(1 - 1/\kappa^2)} [f_{ps}(\mathrm{i} \log \kappa) f_{sp}(-\mathrm{i} \log \kappa) + f_{sp}(\mathrm{i} \log \kappa) f_{ps}(-\mathrm{i} \log \kappa)],\end{aligned} \tag{3.8}$$

where $\kappa = k_{sv}^b / k_p^b$. $f_{qt}(\theta)$ $(q, t = p, s)$ are the far-field forms of an individual scatterer and can be obtained by

$$f_{pp}(\theta) = \sum_{m=-\infty}^{\infty} B_m^{pp} \mathrm{e}^{\,\mathrm{i}\, m\theta} \mathrm{e}^{\,-\mathrm{i}\, m\frac{\pi}{2}}, \tag{3.9}$$

$$f_{ps}(\theta) = \sum_{m=-\infty}^{\infty} C_m^{ps} \mathrm{e}^{\,\mathrm{i}\, m\theta} \mathrm{e}^{\,-\mathrm{i}\, m\frac{\pi}{2}}, \tag{3.10}$$

$$f_{sp}(\theta) = \sum_{m=-\infty}^{\infty} B_m^{sp} \mathrm{e}^{\,\mathrm{i}\,m\theta} \mathrm{e}^{\,-\mathrm{i}\,m\frac{\pi}{2}}, \tag{3.11}$$

$$f_{ss}(\theta) = \sum_{m=-\infty}^{\infty} C_m^{ss} \mathrm{e}^{\,\mathrm{i}\,m\theta} \mathrm{e}^{\,-\mathrm{i}\,m\frac{\pi}{2}}. \tag{3.12}$$

B_m^{qt} and C_m^{qt} are the expansion coefficients of scattered P- and SV-waves for the incident P- and SV-waves, respectively. The forward scattering amplitude $f_{qt}(0)$ $(q, t = p, s)$ can be given as

$$f_{pp}(0) = \sum_{m=-\infty}^{\infty} (-\mathrm{i}\,)^m B_m^{pp}, \tag{3.13}$$

$$f_{ps}(\theta) = \sum_{m=-\infty}^{\infty} (-\mathrm{i}\,)^m C_m^{ps}, \tag{3.14}$$

$$f_{sp}(\theta) = \sum_{m=-\infty}^{\infty} (-\mathrm{i}\,)^m B_m^{sp}, \tag{3.15}$$

$$f_{ss}(0) = \sum_{m=-\infty}^{\infty} (-\mathrm{i}\,)^m C_m^{ss}. \tag{3.16}$$

The normalized effective velocity and attenuation can be obtained by

$$c_p^*/c_p^b = k_p^b/\mathrm{Re}(k_p^*), \tag{3.17}$$

$$c_{sv}^*/c_{sv}^b = k_{sv}^b/\mathrm{Re}(k_{sv}^*), \tag{3.18}$$

$$\alpha_p^b = \mathrm{Im}(k_p^*/k_p^b), \tag{3.19}$$

$$\alpha_{sv}^b = \mathrm{Im}(k_{sv}^* k_{sv}^b/k_{sv}^b). \tag{3.20}$$

Let us consider a fictitious homogeneous material which has the same dispersive properties (frequency-dependent effective propagation speed) as the considered composites. Then, the fictitious homogeneous material should have the frequency-dependent elastic moduli. These effective dynamic elastic moduli can be expressed as

$$\frac{\mu_t^*}{\mu_t^b} = \frac{\rho^*}{\rho^b}\left[\mathrm{Re}\left(\frac{k_{sv}^b}{k_{sv}^*}\right)\right]^2, \tag{3.21}$$

$$\frac{K^*}{K^b} = \frac{\rho^*}{\rho^b}\left\{\left(\mathrm{Re}\left(\frac{k_p^b}{k_p^*}\right)\right)^2 + \frac{\mu_t}{K}\left[\left(\mathrm{Re}\left(\frac{k_p^b}{k_p^*}\right)\right)^2 - \left(\mathrm{Re}\left(\frac{k_{sv}^b}{k_{sv}^*}\right)\right)^2\right]\right\}, \tag{3.22}$$

where the effective density will be obtained from the simple rule of mixture $\rho^* = c\rho^f + (1-c)\rho^b$, μ_t^b and K^b $(= \lambda^b + \mu^b)$ are the transverse shear modulus and plane-strain bulk modulus of the host, respectively, and μ_t^* and K^* denote the effective dynamical elastic moduli.

4. Numerical results and discussion

Atomic simulations demonstrated that the elastic constants λ^s and μ^scan be either positive or negative, λ^s/μ^b and μ^s/μ^b are in the order of angstroms [20]. For a macroscopic fiber, the parameter S_1 is thus close to zero. The surface effects can be neglected and Eq. (2.25) reduces to the solution of the classical elasticity theory. However, the parameter S_1 becomes large enough and the surface effects should be considered when the radius of cylindrical fiber a shrinks to nanometers scale. It is noted from the expressions of S_1 and S_2 that S_2 is much smaller than S_1 at the nanometer scale. The influence of S_2 is nearly unnoticeable at nanometer scale. Therefore, the influence of S_1 is the main concern. In the following numerical examples, the host material is assumed to be isotropic aluminum ($\rho^b = 2700$ kg/m^3, $\mu^b = 34.7$ (GPa), $K^b = 75.2$ (GPa)). Two types of fiber, namely, the soft fiber ($g = \mu^f/\mu^b = 0.5$, $K^f/K^b = 0.5$) and the stiff fiber ($g = \mu^f/\mu^b = 2$, $K^f/K^b = 2$), are discussed. The fiber is supposed to have the same Poisson ratio as the host material, and the density ratio is kept fixed in the numerical simulation, i.e., $\rho^f/\rho^b = 1.2$. The selected volume fraction $c = 0.3$ is considered in the numerical examples.

Figures 2 and 3 show the surface effects on the effective velocity and the effective attenuation of coherent P-wave. It is found that the effective velocity increases gradually with the increase of surface parameter S_1 both for soft fiber and for stiff fiber. However, the effective attenuation decreases gradually for the soft nanofiber and increases gradually for the stiff fiber with the increase of surface parameter S_1. Usually, the elastic constants of macroscale material are positive values. The surface/interface may have elastic constants of negative value due to the unique microstructure of surface/interface. It is observed that

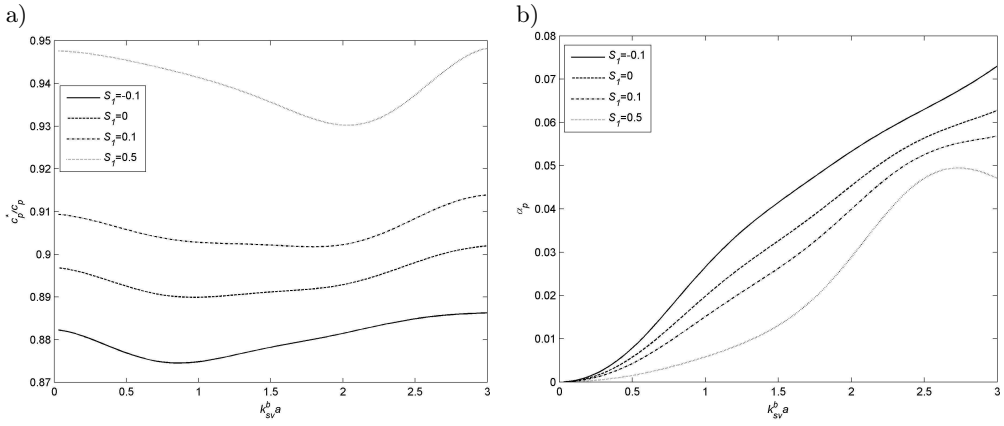

FIG. 2. Effective velocity and attenuation of coherent P-wave in composites with soft fibers at different surface parameters S_1; a) effective velocity, b) effective attenuation.

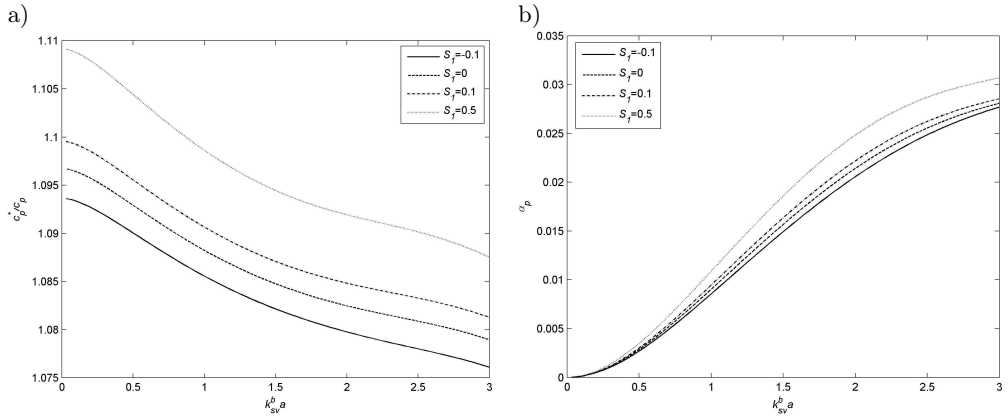

FIG. 3. Effective velocity and attenuation of coherent P-wave in composites with stiff fibers at different surface parameters S_1; a) effective velocity, b) effective attenuation.

the influences of negative surface parameter show an opposite trend to that of the positive surface parameter.

Figures 4 and 5 show the surface effects on the effective velocity and effective attenuation of coherent SV-wave. Similarly to the coherent P-wave, the effective velocity of coherent SV-wave increases due to the surface effects for both the soft fiber and the stiff fiber. The effective attenuation undergoes an opposite change for the soft and stiff fibers. However, there is something different from the coherent P-wave. Consider that $k_{sv}^b a = \omega a/c^b$, the increase of $k_{sv}^b a$ means the increase of the frequency ω for the fixed radius of fiber. It is observed that the surface effects on the effective speed of coherent SV-wave are

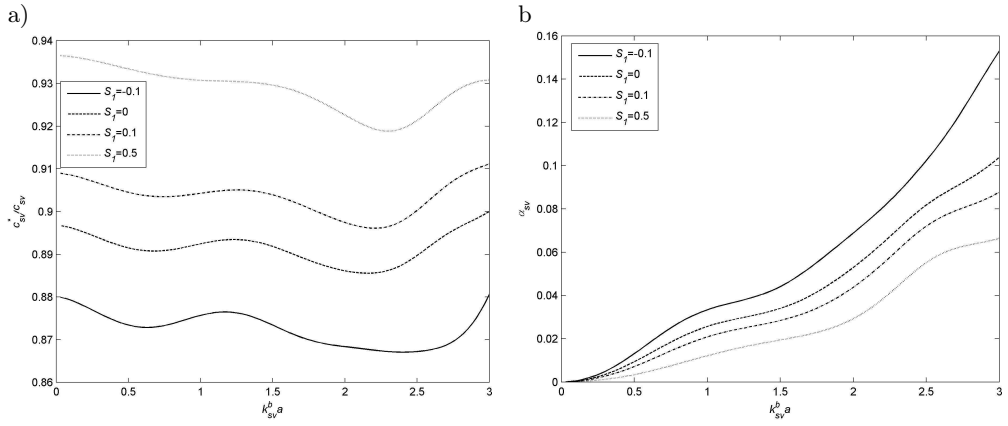

FIG. 4. Effective velocity and attenuation of coherent SV-wave in composites with soft fibers at different surface parameters S_1; a) effective velocity, b) effective attenuation.

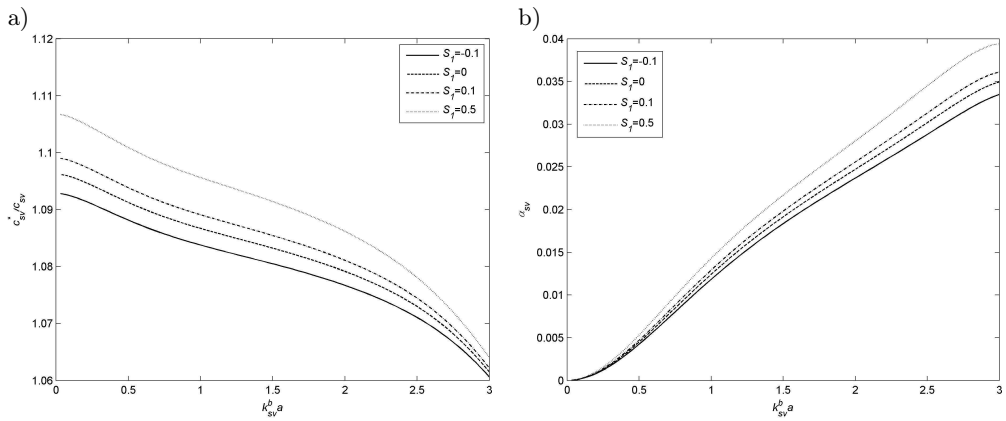

FIG. 5. Effective velocity and attenuation of coherent SV-wave in composites with stiff fibers at different surface parameters S_1; a) effective velocity, b) effective attenuation.

more evident at lower frequency than at higher frequency for both the soft fiber and the stiff fiber. But the surface effects is nearly the same at lower frequency and at higher frequency for the coherent P-wave. The surface effects on the attenuation coefficient have evident frequency dependence, namely, the surface parameter has more evident influence on the attenuation coefficient at higher frequency.

Figures 6 and 7 show the effective dynamic transverse shear modulus and effective dynamic bulk modulus of composite material. The surface effects on the effective dynamical elastic moduli are more evident for the composite material with soft nanofibers in comparison with the composite with stiff fibers. Moreover,

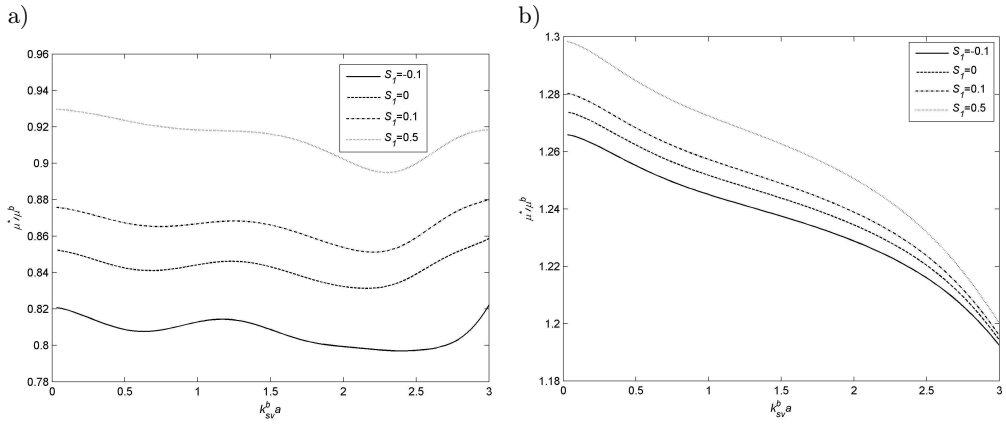

FIG. 6. Effective dynamic transverse shear modulus of composite material at different surface parameters S_1; a) soft fibers, b) stiff fiber.

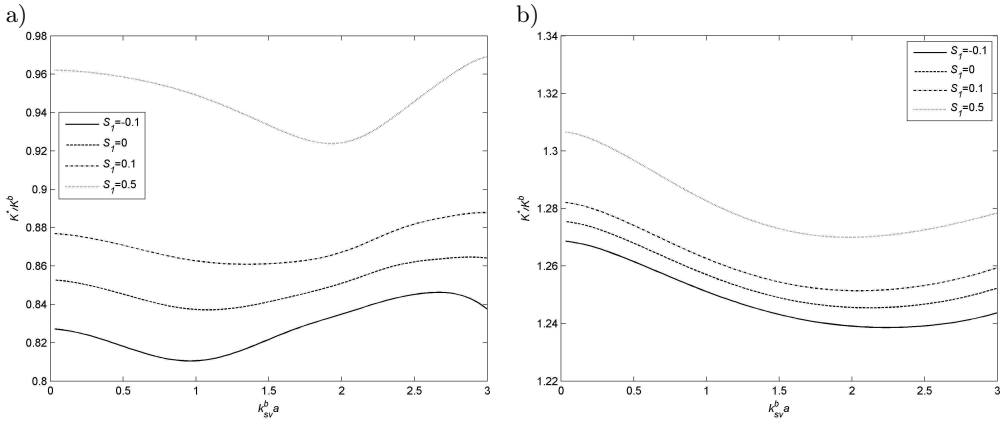

Fig. 7. Effective dynamic bulk modulus of composite material at different surface parameters S_1; a) soft fiber, b) stiff fiber.

the effective dynamical transverse shear modulus has more evident frequency dependence than the effective bulk modulus.

5. Conclusions

The effective velocity and the effective attenuation of coherent waves exhibit evident dependence on the surface parameter. In general, the effective velocity increases due to the surface effects both for soft nanofiber-reinforced and for stiff nanofiber-reinforced composites. However, the effective attenuation decreases for soft fiber-reinforced composites but increases for stiff fiber-reinforced composites due to the surface effects. Moreover, the effective velocity of coherent SV-wave exhibits more evident dependence on the surface parameter at a lower frequency than at a higher frequency for both of the composites with soft and stiff fibers while the effective velocity of coherent P-wave exhibits the same dependence at lower and higher frequencies in considered frequency range. The dependences of effective attenuation on the surface parameter are more evident at higher frequency than at lower frequency for both of the composites with soft and stiff fiber. The effective dynamical elastic moduli are also frequency dependent and exhibit similar trend with the effective velocity. The surface effects on the effective dynamical elastic moduli are also more evident for the composite material with soft fibers in comparison with the composite with stiff fibers.

Acknowledgement

The work is supported by the National Natural Science Foundation of China (No. 10972029) and Opening Fund of State Key Laboratory of Nonlinear Mechanics (LNM), in Institute of Mechanics, Chinese Academy of Sciences.

References

1. D.Y. LI, J.A. SZPUNAR, *Determination of single crystals' elastic constants from the measurement of ultrasonic velocity in the polycrystalline material*, Acta Metallurgica et Materialia, **40**, 12, 3277–3283, 1992.
2. Y.-C. LEE, J.O. KIM, J.D. ACHENBACH, *Acoustic microscopy measurement of elastic constants and mass density*, Ultrasonics, Ferroelectrics, and Frequency Control, **42**, 2, 253–264, 1995.
3. V. GIURGIUTIU, A. CUC, *Embedded non-destructive evaluation for structural health monitoring, damage detection, and failure prevention*, The Shock and Vibration Digest, **37**, 2, 83–105, 2005.
4. X. LIU, P. WEI, *Estimation of interface damage of fiber-reinforced composites*, Mechanics of Composite Material, **44**, 1, 37–44, 2008.
5. M.-H. LU, L. FENG, Y.-F. CHEN, *Phononic crystals and acoustic metamaterials*, Materials Today, **12**, 12, 34–42, 2009.
6. S.K. BOSE, A.K. MAL, *Axial shear waves in a medium with randomly distributed cylinders,* Journal of the Acoustical Society of America, **55**, 519-523, 1974.
7. S.K. BOSE, A.K. MAL, *Elastic waves in a fiber-reinforced composite*, Journal of the Mechanics and Physics of Solids, **22**, 217–229, 1974.
8. S.K. BOSE, A.K. MAL, *Longitudinal shear waves in a fiber-reinforced composite*, International Journal of Solids and Structures, **9**, 1075–1085, 1973.
9. R.B. YANG, A.K. MAL, *Multiple scattering of elastic waves in a fiber-reinforced composite*, Journal of the Mechanics and Physics of Solids, **42**, 1945–1968, 1994.
10. Y. SHINDO, N. NIWA, *Scattering of antiplane shear waves in a fiber-reinforced composite medium with interfacial layers*, Acta Mechanica, **117**, 181–190, 1996.
11. Y. SHINDO, N. NIWA, R. TOGAWA, *Multiple scattering of antiplane shear waves in a fiber-reinforced composite medium with interfacial layers*, International Journal of Solids and Structures, **35**, 7, 733–745, 1998.
12. P.J. WEI, Z.P. HUANG, *Dynamic effective properties of the particle-reinforced composites with the viscoelastic interphase*, International Journal of Solids and Structures, **41**, 24-25, 6993–7007, 2004.
13. P.J. WEI, *A self-consistent approach to the dynamic effective properties of composites reinforced by distributed spherical particles*, Acta Mechanica, **185**, 67–79, 2006.
14. M.E. GURTIN, A.I. MURDOCH, *A continuum theory of elastic material surfaces*, Archive for Rational Mechanics and Analysis, **57**, 291–323, 1975.
15. Y. RU, G.F. WANG, T.J. WANG, *Diffractions of elastic waves and stress concentration near a cylindrical nano-inclusion incorporating surface effect*, Journal of Vibration and Acoustics, **131**, 061011, 2009.
16. F.W. QIANG, P.J. WEI, L. LI, *The effective propagation constants of SH wave in composites reinforced by dispersive parallel nanofibers*, Science China Physics, Mechanics & Astronomy, **55**, 7, 1172–1177, 2012.

17. S.M. HASHEMINEJAD, R. AVAZMOHAMMADI, *Size-dependent effective dynamic properties of unidirectional nanocomposites with interface energy effects*, Composite Sciences and Technology, **69**, 2538–2546, 2009.

18. C.M. LINTON, P.A. MARTIN, *Multiple scattering by random configurations of circular cylinders: second-order corrections for the effective wavenumber*, Journal of the Acoustical Society of America, **117**, 6, 3413–3423, 2005.

19. J.M. CONOIR, A.N. NORRIS, *Effective wave numbers and reflection coefficients for an elastic medium containing random con?gurations of cylindrical scatterer*, Wave Motion, **47**, 183–197, 2010.

20. V.B. SHENOY, *Atomistic calculations of elastic properties of metallic fcc crystal surfaces*, Physical Review B, **71**, 1–14, 094104, 2005.

21. L. PLACIDI, G. ROSI, I. GIORGIO, A. MADEO, *Reflection and transmission of plane waves at surfaces carrying material properties and embedded in second-gradient materials*, Mathematics and Mechanics of Solids, **19**, 5, 555–578, 2014.

22. D.J. STEIGMANN, R.W. OGDEN, *Plane deformations of elastic solids with intrinsic boundary elasticity*, [in:] Proceedings of The Royal Society of London, Series A, **453**, 1959, 853–877, 1997.

Received December 18, 2014; revised version June 16, 2015.